Pure Appl. Chem., Vol. 84, No. 11, pp. 2299–2308, 2012.
http://dx.doi.org/10.1351/PAC-CON-12-01-05

Nanotechnology-driven chemistry of boron materials*

Amartya Chakrabarti and Narayan S. Hosmane‡

Department of Chemistry and Biochemistry, Northern Illinois University, DeKalb, IL 60115, USA

Abstract: The chemistry and reactivity of carborane-appended magnetic nanoparticles and boron-based nanomaterials are briefly reviewed with an emphasis on our contribution to this field. The carborane-appended magnetic nanoparticles exhibited great potential to be useful in boron neutron capture therapy (BNCT). A facile route to synthesize boron nanorods (BNRs) and boron nitride nanotubes (BNNTs) is also demonstrated. While functionalized BNRs and BNNTs have been successfully prepared, the derivatives of BNNTs were investigated as potential carriers for BNCT.

Keywords: biomedical applications; boron; boron nanomaterials; boron neutron capture therapy (BNCT); carboranes; magnetic nanoparticles.

INTRODUCTION

Boron clusters have been traditionally used in organometallic chemistry as metal binding ligands, in catalysis, and in medicine as a source of boron atoms. More recently, they have been used in various materials science applications. A number of unique properties of boron clusters such as high thermal and chemical stability, ease of functionalization, three-dimensional structure, aromaticity, and special electronic properties have been instrumental for their use in materials science. Some of the recent uses of boron clusters have been in luminescent materials, polymers, coordination polymers, nanoscience, dendrimers, liquid crystals, and nonlinear optics.

Although classical heterogeneous catalysts, normally in micrometer scale, have been widely used in industries [1,2], significant decrease in activity or selectivity is commonly observed owing to steric and diffusion factors [1]. A major portion of these catalysts is present deep inside the support matrixes restricting limited access of the reactants to the catalytic sites [1]. On the other hand, both nano-scaled metal-based catalyst and support material were probed to improve the activity and selectivity of catalysts [3]. When the size of the support materials is decreased to nanometer scale, the surface area is substantially increased and the support can be evenly well-dispersed in solution, forming a homogeneous emulsion [2,3]. Furthermore, nanoparticles do not suffer from porosity and other associated problems with transport of reactant and/or product to and from the catalyst. Nonetheless, during the recovery and recycling of catalyst from this immobilized system, similar problems are still encountered. Therefore, an efficient technique for facile separation of catalyst was warranted, and hence, magnetic property was introduced.

Pure Appl. Chem.* **84, 2183–2498 (2012). A collection of invited papers based on presentations at the 14th International Meeting on Boron Chemistry (IMEBORON-XIV), Niagara Falls, Canada, 11–15 September 2011.
‡Corresponding author

Recently, the idea of using magnetic nanoparticles as alternative catalyst support has been extensively employed in view of their high surface area yielding to high catalyst loading capacity, high dispersion, outstanding stability, and convenient catalyst recycling [4]. Magnetically driven separation makes the recovery of catalysts in liquid-phase reaction much easier than by cross-flow filtration and centrifugation. As the catalysts are usually immobilized on the surface of nanoparticles, easy access by reactants to the active sites can also be achieved. Comparison has been done among immobilizing supports with different sizes in order to study the dependency of catalytic activity on supports sizes, and the results indicated that nano-scaled supports gave the highest regioselectivity and product yield [5].

It is obvious that tremendous improvement has been achieved in the preparation and application of magnetic nanoparticle-supported catalysts for various organic transformations [6]. However, the synthesis and stabilization of monodispersed magnetic nanoparticles with controllable size remain a big challenge. The use of magnetic nanoparticles in catalytic applications has been a major development at the frontiers of both symmetric and asymmetric catalyses. To date, remarkable progress has been made on magnetic nanoparticle-based catalyst system from the activity and recyclability standpoints. The unavoidable limitation associated with the intrinsic instability of magnetic nanoparticles over a long period of time has to be addressed in order to enhance the reusability of the supported catalysts and thus minimize the cost of the catalyst precursors. Stabilization and surface functionalization of magnetic nanoparticles remain an active area of research that will undoubtedly bring more applications not only in organic synthesis, but in biomedical research as well.

In the last few decades, pure boron as well as boron-based nanomaterials emerged with great potential in various fields of applications [7]. Boron nanomaterials possess a variety of interesting properties that are suitable for such diversity. The high surface-to-volume ratio of boron nanoparticles coupled with boron's high energy content make such nanoparticles attractive as fuel additives in conventional hydrocarbon fuels for air-breathing propulsion systems. Their robust thermal and electrical stabilities, compared to metal nanowires, make one-dimensional boron nanostructures, such as nanowires, nanorods, nanobelts, or nanotubes, promising materials for nanoscale electrically conducting interconnects in nanoelectronic devices. Boron-based nanoparticles are now being extensively investigated as a boron source in boron neutron capture therapy (BNCT).

CHEMISTRY AND BIODISTRIBUTION STUDIES OF CARBORANE-APPENDED MAGNETIC NANOPARTICLES

Commercially available magnetic nanoparticles of iron oxides matrixed with starch have been enriched with the carborane cages, 1-R-2-butyl-*ortho*-$C_2B_{10}H_{10}$ (R=Me, **3**; Ph, **4**), by catalytic azide-alkyne cycloaddition reactions [8]. This reaction has been extensively developed and widely used in chemical transformations in biological applications and materials chemistry [9], such as cell surface labeling [10], biopolymers–viruses conjugation [11], and block copolymer synthesis [12].

Specifically, starch-modified magnetic nanoparticles were enriched with propargyl groups by reactions of free hydroxyl groups in starch with propargyl bromides in dimethylformamide (DMF) in the presence of sodium hydroxide (Scheme 1) [8]. There were no significant changes in the IR spectra before and after immobilization of propargyl groups. However, after immobilizing the carborane cages, a new peak appeared at $\nu = 2575$ cm^{-1}, assigned to the B–H bond stretching. Compared with the starting compound 1-Me-2-$(CH_2)_4N_3$-1,2-$C_2B_{10}H_{10}$, the absorption of $\nu_{N\equiv N}$ at 2097 cm^{-1} disappeared in IR spectra of **3**. These results confirm the successful immobilization of propargyl and carborane groups [8]. The successive attachments are consistent with the thermal gravimetric analysis (TGA) of compounds **1**, **2**, and **3**, the curves indicate a wt % loss of 27.7 and 33.2 for **1** and **2**, respectively, while compound **3** has a much smaller loss of 15.7 %. For the propargyl group, a loading amount of 1.40 mmol per gram of starch-matrixed magnetic nanoparticles has been reached based on TGA and elemental analyses [8]. Unfortunately, the absence of TGA of **3** prevented the determination of the loading

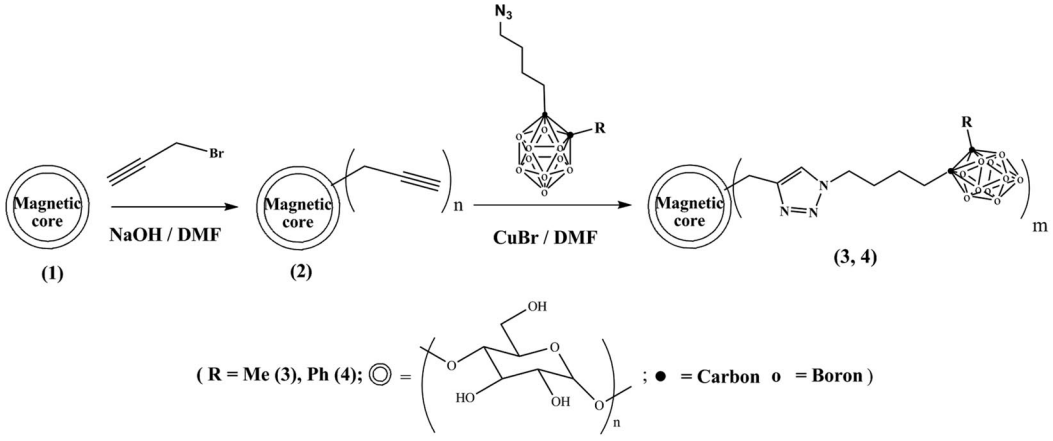

Scheme 1 Synthesis of encapsulated magnetic nanocomposites.

amounts of carborane. However, the inductively coupled plasma optical-emission spectroscopy (ICP-OES) analysis was decisive in obtaining a loading amount of 9.83 mmol boron atom/g starch-matrixed magnetic nanoparticles.

It should be pointed out that, after modification, the transmission electron microscopy (TEM) image of **3** (Fig. 1a), showed that aggregation of the modified magnetic nanoparticles had occurred, which may be caused by solvent evaporation of TEM samples. This phenomenon has been generally reported [13–15]. In contrast, most of the magnetic nanoparticles of **3** have been found separated in the atomic force microscope (AFM) image (Figs. 1d,e).

The resulting nanocomposites have been found to be highly tumor-targeted vehicles under the influence of external magnetic field (1.14T), giving a high boron concentration of 51.4 μg/g tumor and high ratios of around 10:1 tumor-to-normal tissues (Fig. 2) [8]. Nonetheless, using "click" reaction, carborane cages have been successfully attached to modified magnetic nanoparticles for the first time. The resulting nanocomposites have been found to accumulate in tumor cells in high concentration in the presence of external magnetic field. These results provide new hope for the research of neutron capture therapy (NCT) and the combination of the drugs with BNCT/MRI/thermotherapy characteristics. More complete biodistribution and cytotoxicity studies are currently underway in our laboratories.

These results have significance in the treatment of not only brain tumors, but for other kinds of cancers through BNCT. This research is just in its initial stages, and issues related to magnetic nanoparticles, such as particle size control, surface functionalizations, and their environmental compatibility need to be addressed.

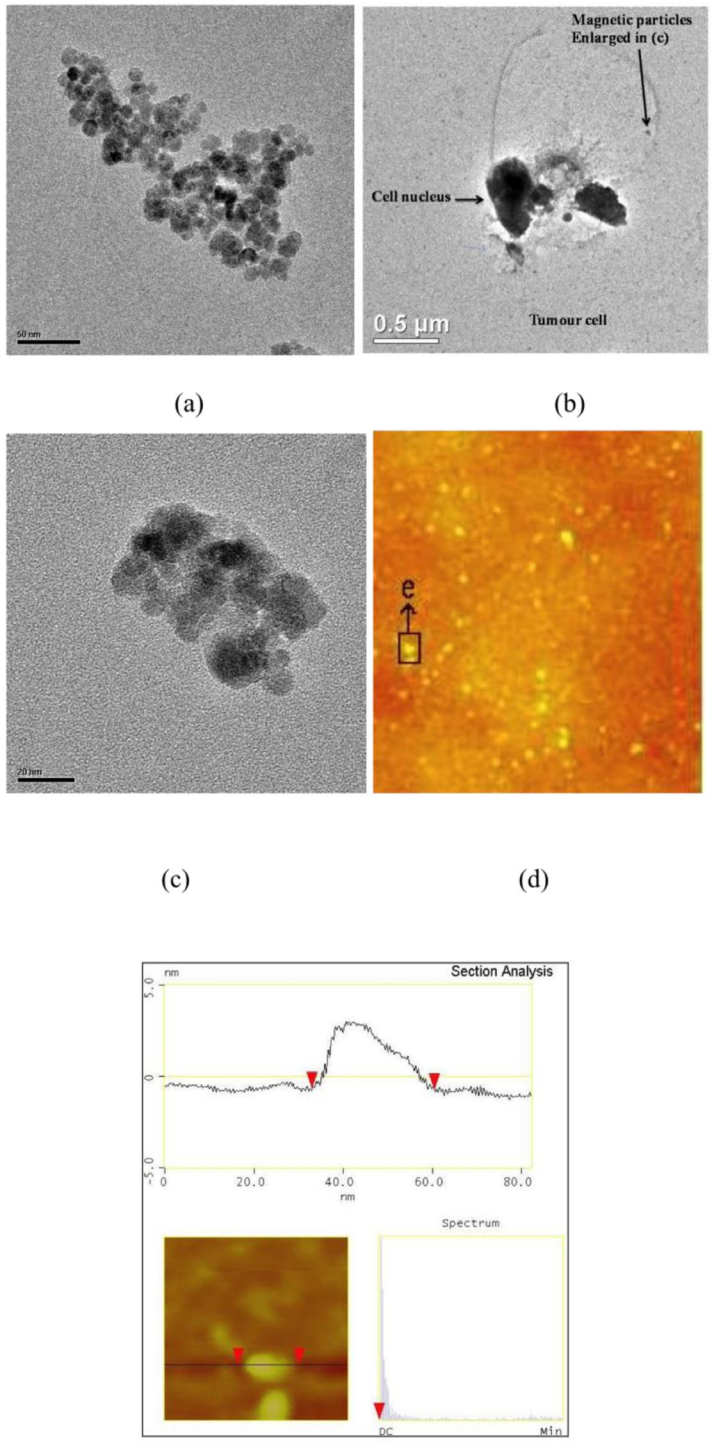

Fig. 1 TEM images showing the magnetic cores of compound **3**; free (a), inside tumor cells (b, c), and AFM (d, e).

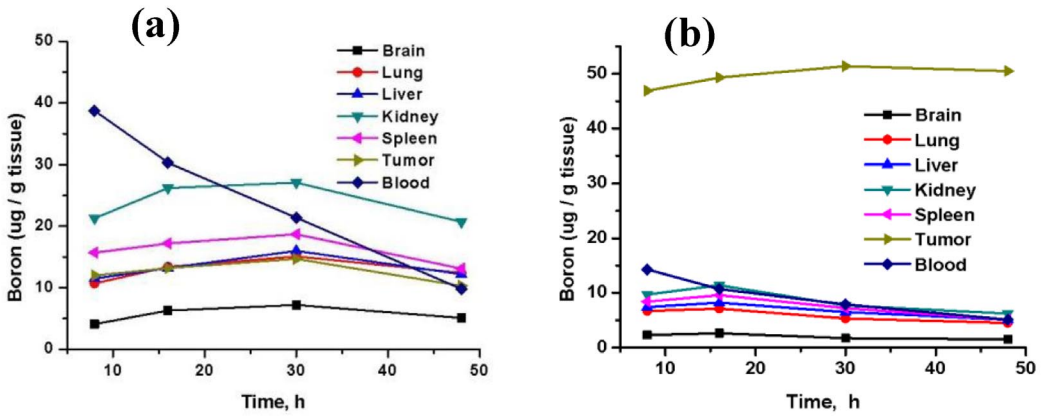

Fig. 2 Boron tissue distribution of **3**, (a) without external magnet, (b) with external magnet.

Syntheses and reactivity of boron nanorods (BNRs) and boron nitride nanotubes (BNNTs)

Synthesis of BNRs

Nanorods are fundamentally the miniature version of nanowires, typically grown via similar methods used for nanowires. They have excellent potential to be useful as seed materials for several boron-based nanostructures. Boron nanostructures have the unique ability to maintain the same properties of boron as in bulk, while carrying the advantages of nanodimensions. Such advantages include a higher surface-to-volume ratio, which may increase the catalytic activities of certain nanomaterials [16]. Additionally, with the high surface-to-volume ratio of boron nanoparticles, and boron's high energy content, they can be used as a fuel additive in conventional hydrocarbon fuels for air-breathing propulsion systems [17,18]. Nanodimensions are also effective and sought-after because of their spatial confinement and reduced number of structural defects, which may improve mechanical properties and chemical stabilities [16]. Compared to bulk boron, boron nanowires show higher conductivities, allowing them to be usable as building blocks for flexible nanoelectronics [16]. Boron-doped diamond nanopowder is currently synthesized and used as electrocatalyst support material and electrode materials. In comparison to other metal nanowires, the electrical and thermal stability of boron nanostructures make them capable of producing nanoscale electrically conducting interconnects in nanoelectronic devices [19,20]. The future looks toward boron-based nanomaterials to be used more as a boron source in BNCT [21].

To date, most of the boron-based nanomaterials have been synthesized using either drastic reaction conditions or toxic precursors [22–24]. A simple methodology has recently been developed to prepare nanostructures of boron materials from nontoxic boron oxide smelted in liquid lithium (eq. 1) [25].

$$B_2O_3\,(s) + 6Li\,(l) \xrightarrow[\text{Ultrasound}]{\text{Smelting at } 250\ ^\circ C} 2B\,(s) + 3Li_2O\,(s) \xrightarrow[B_2O_3\,(s)\text{ and by-product } Li_2O\,(s)]{\text{Leaching off unreacted Li } (s) \text{ and}} BNRs(s) \quad (1)$$

In the preparatory process of the BNRs, the purification part was the key to the synthetic success. Apparently, it was crucial to avoid any formation of lithium borides in the synthesis or at least destroy such a contaminant in the product with proper treatment and washing sequences. According to some earlier work by Serebryakova et al., lithium diboride is not very stable and is easily soluble in methanol; it also decomposes in weak mineral acid solutions [26]. On the other hand, lithium tetraboride is not stable in potassium hydroxide solution. Thus, these observations guided the purification protocol applied in the synthesis of the BNRs described above. Methanol was first added after completion of the reaction to avoid the vigorous reaction of water with lithium. One of the reasons for not washing the

product immediately with water is to avoid the formation of lithium hydroxide that is capable of etching the nickel crucible. B_2O_3, being soluble in hot water, was easily removed by washing with hot water. While the potassium hydroxide solution was used to remove any lithium tetraboride, dilute HCl solution was used to take away the lithium diborides, if any, as well as to neutralize the basic condition of the solution. Washings were repeated until the product was free of any residual acid [25].

The TEM images of the resulting boron materials are shown in Fig. 3. Apparently, the dominant feature is the rod-like structures (Fig. 3a). The preferential formation of BNRs over nanoparticles must be associated with the streaming-like ultrasonic propagation [27,28], which can transfer acoustic momentum efficiently to the liquid lithium [29], leading to a sort of directed lithiation in a B_2O_3 powder. While in a random insertion of lithum, the dominant resulting structure of boron is believed to be nanoparticles. The TEM images also suggest that the diameters of most of the nanorods exhibit a fairly narrow distribution, ranging between 20~40 nm. The length of the rods varies, and most of the length of the nanorods falls in the region between 80 and 200 nm, but there are some longer nanorods of more than 500 nm (Fig. 3b). Some spherical boron nanoparticles embedded in the BNRs (Fig. 3c) were also observed. Nonetheless, BNRs were produced in good yields (85 %) from B_2O_3 by this ultrasonic smelting method. This simple and greener process neither involves any harmful and toxic boron precursors nor does it require any severe reaction conditions.

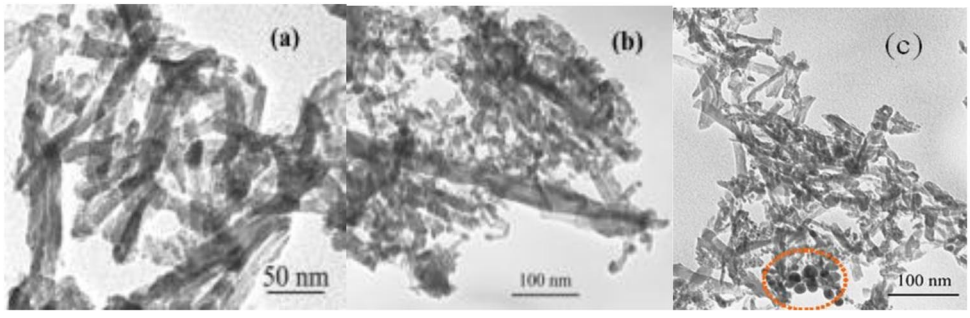

Fig. 3 TEM images of BNRs showing abundant nanorod formation of varying length and diameters (a) bundles of nanorods; (b) some long nanorods; (c) nanorods of shorter lengths and the spherical boron nanoparticles (highlighted in the circular part).

The products were thoroughly characterized using Fourier transform infrared (FT-IR) spectroscopy, UV–vis spectroscopy, and TEM. Even though this work demonstrates an alternative nonhazordous route for large-scale synthesis of boron nanomaterials at low temperature, a further study on obtaining narrower size distribution of the rods using controlled ultrasonication during the mixing process is warranted and carried out concurrently.

Water solubility of BNRs

The success of BNRs in BNCT depends mostly on their solubility in water. A unique methodology to prepare water-soluble BNRs via interaction with amine-terminated polyethylene glycol has been investigated in our laboratories [30]. Earlier research has shown that the BNNTs can be solubilized using such polymers taking advantage of the interaction between amine groups of the polymers with electron-deficient boron atoms of the nanomaterials [31]. Thus, the BNRs were allowed to react with the polymer for 3 days at 100 °C. After that, water has been added to the mixture and the reaction was carried out for another 24 h under reflux. With completion of the reaction, the mixture was centrifuged several times to recover any of the unreacted BNRs. The resulting clear yellow solution did not show any precipitation after being kept for several days. The solution was then evaporated and dried in vacuo to isolate a solid residue. The TEM of the residue confirmed the presence of soluble nanorods in the product

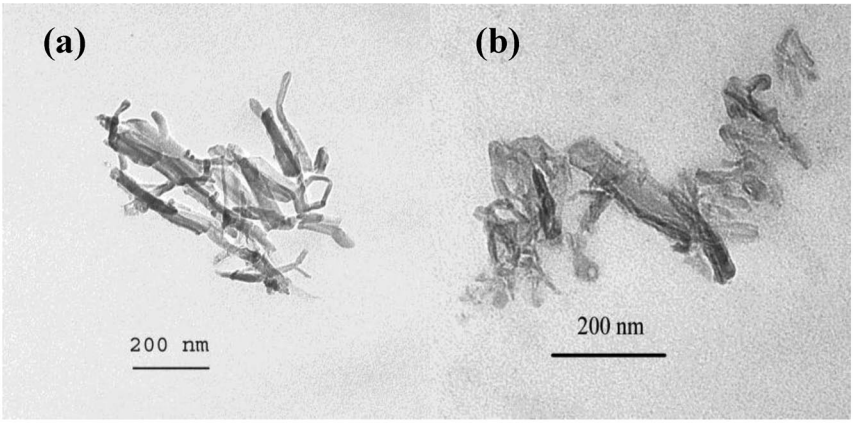

Fig. 4 TEM image of (a) BNRs; (b) water-soluble BNRs.

(Fig. 4). Further characterization of the product is currently in progress. Biodistribution studies of the new product are currently being performed to ensure its utility elsewhere.

Synthesis and functionalization of BNNTs

BNNTs found their application in several fields, since their first synthesis by Chopra et al. in 1995 [32]. They are suitable for mechanical and electronic devices by virtue of their excellent mechanical, thermal, and electrical properties [33]. They are chemically inert and stable toward oxidation up to 900 °C, unlike their carbon counterpart, carbon nanotubes (CNTs) [34]. The most commonly used methods for preparation of BNNTs include arc discharge methods [35], chemical vapor deposition techniques [36], laser ablation methods [37], mechano-thermal methods [38], and other chemical syntheses [39]. Most of them use drastic reaction conditions like high temperature, in the range of 1000 °C or more, and require expensive and complicated reaction set-ups. Work by Smith et al. reported large-scale production of BNNTs at 4000 °C [40]. In addition, Xu and co-workers described a simpler technique of pyrolysis in an autoclave to produce BNNTs using an Fe/Zn catalytic mixture at lower temperatures [41]. The method is effective, yet not efficient enough since the product is hard to purify. The gray product obtained from this process contained a significant amount of the catalyst.

Since the synthesis of BNNTs in autoclave is a simple and comparatively lower temperature method, we investigated a different catalyst system following similar reaction protocols. Among several group 1 and group 2 metals, magnesium (Mg) has been proven to be useful to produce BNNTs in large scale. It is much easier to purify the product since Mg forms a chloride when treating the compounds with hydrochloric acid. The products have been repeatedly washed with 6N HCl and then with deionized water to remove the chlorides and the acid. The purified white product was characterized via FT-IR spectroscopy (Fig. 5) and TEM (Fig. 6) [42].

The FTIR data clearly exhibits the evidences of formation of hexagonal boron nitride (the peaks at 1380 and 810 cm^{-1}), while the TEM images show abundant presence of nanotubes in the product along with a very few nanocages. Interestingly, we have seen a reduction in the amount of cages with an increment of reaction temperature from 600 to 800 °C [42]. Further characterization of the product and studies on the dependence of the product properties on catalyst size and temperature of the reaction are currently underway in our laboratories.

Although BNNTs are isoelectronic with CNTs, their biomedicinal applications were not explored in detail. Insolubility of BNNTs, not only in aqueous media but also in most organic solvents, remained a major issue that can be addressed if they are functionalized. Both covalent and noncovalent functionalizations of BNNTs have been reported recently. While BNNTs, wrapped in a polymer, were soluble in organic solvents such as chloroform and tetrahydrofuran [43], the interactions with amine-terminated

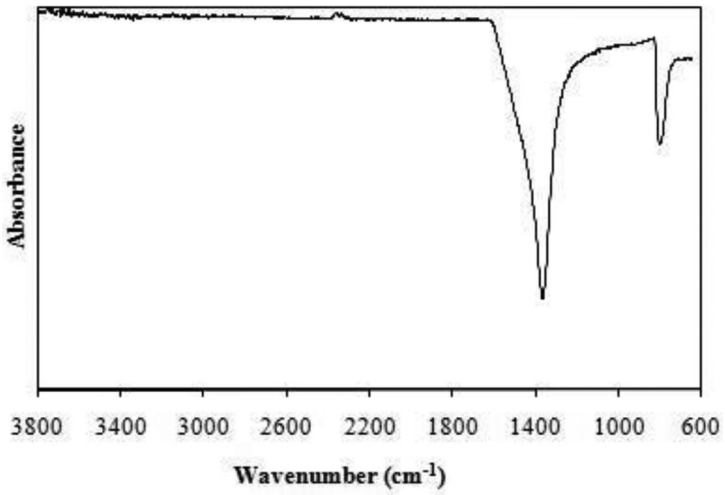

Fig. 5 FTIR spectrum of BNNTs.

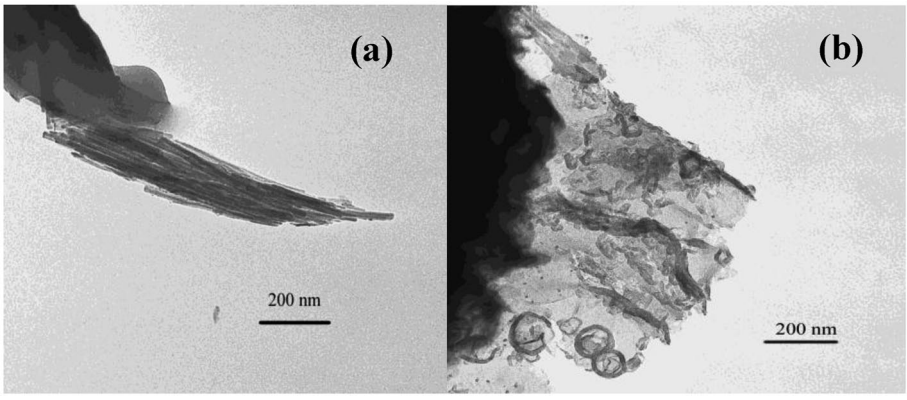

Fig. 6 TEM Images of (a) BNNTs, and (b) BNNTs with some nanocages.

oligomeric poly(ethylene glycol) [31], stearoyl chloride [44], Lewis bases [45], as well as their ammonia plasma irradiation [46] have been investigated to functionalize the BNNTs. Nevertheless, the non-cytotoxic nature of BNNTs warrants their further investigation for use in BNCT [47].

CONCLUSIONS

A number of methodologies have been investigated to integrate carborane clusters into a variety of materials, including nanostructured cages, rods, tubes, and magnetic composites. When carboranes are bonded to supports, the resulting products showed promise to be the novel therapeutic and/or catalytic materials. The research on BNRs and BNNTs, a counterpart to the more widely studied single-walled CNTs, was found to be a worthwhile investigation. Thus, the carborane cage-appended nanocomposites showed a great potential to be the tumor-targeting vehicles. On the other hand, the full potential of purely boron-based nanomaterials such as BNRs and BNNTs is yet to be explored and such studies are currently underway in our laboratories. Nonetheless, the greener route to synthesize these materials is the highlight of this study and will continue to be the focal point of our research.

ACKNOWLEDGMENTS

This work was supported by grants from the National Science Foundation (CHE-0906179 and CHE-0840504), Kishwaukee Community Hospital, Alexander von Humboldt Foundation, and the NIU Inaugural Board of Trustees Professorship Award.

REFERENCES

1. H. F. Rase. *Handbook of Commercial Catalysts: Heterogeneous Catalysts*, CRC Press, New York (2000).
2. T. J. Yoon, W. Lee, Y.-S. Oh, J.-K. Lee. *New J. Chem.* **27**, 227 (2003).
3. (a) Y. Zhu, C. N. Lee, R. A. Kemp, N. S. Hosmane, J. A. Maguire. *Chem. Asian J.* **3**, 650 (2008); (b) A. Didier, F. Lu, J. R. Aranzaes. *Angew. Chem., Int. Ed.* **44**, 7852 (2005).
4. D. K. Yi, S. S. Lee, J. Y. Ying. *Chem. Mater.* **18**, 2459 (2006).
5. T. J. Yoon, J. I. Kim, J. K. Lee. *Inorg. Chim. Acta* **345**, 228 (2003).
6. Y. Zhu, L. P. Stubbs, F. Ho, R. Liu, C. P. Ship, J. A. Maguire, N. S. Hosmane. *ChemCatChem* **2**, 365 (2010).
7. A. Chakrabarti, L. M. Kuta, K. J. Krise, J. A. Maguire, N. S. Hosmane. *Boron Science: New Technologies and Applications*, Chap. 20, p. 475, CRC Press, Boca Raton (2011).
8. Y. Zhu, Y. Lin, Y.-Z. Zhu, J. Lu, J. A. Maguire, N. S. Hosmane. *J. Nanomater.* Article ID 409320 (2010).
9. H. C. Kolb, M. G. Finn, K. B. Sharpless. *Angew. Chem., Int. Ed.* **40**, 2004 (2001).
10. A. J. Link, D. A. Tirrell. *J. Am. Chem. Soc.* **125**, 11164 (2003).
11. S. S. Gupta, K. S. Raja, E. Kaltgrad, E. Strable, M. G. Finn. *Chem. Commun.* 4315 (2005).
12. J. A. Opsteen, J. C. M. van Hest. *Chem. Commun.* 57 (2005).
13. J. Zhou, C. Leuschner, C. Kumar, C. K. Hormes, W. O. Soboyejo. *Biomaterials* **27**, 2001 (2006).
14. G. Beaune, B. Dubertret, O. Clément, C. Vayssettes, V. Cabuil, C. Ménager. *Angew Chem., Int. Ed.* **46**, 5421 (2007).
15. C. Bergemann, D. Muller-Schulte, J. Oster, L. Brassard, A. S. Lübbe. *J. Magn. Magn. Mater.* **194**, 45 (1999).
16. G. Cao (Ed). *Nanostructures & Nanomaterials: Synthesis, Properties & Applications*, Imperial College Press (2004).
17. K. Kleiner. *New Scientist* **2522**, 34 (2005).
18. G. Young, K. Sulivan, M. R. Zachariah, K. Yu. *Combust. Flame* **156**, 322 (2009).
19. I. Boustani, A. Quandt, E. Hernández, A. Rubio. *J. Chem. Phys.* **110**, 3176 (1999).
20. A. Gindulyte, W. N. Lipscomb, L. Massa. *Inorg. Chem.* **37**, 6544 (1998).
21. Z. Yinghuai, K. Cheng Yan, J. A. Maguire, N. S. Hosmane. *Curr. Chem. Biol.* **1**, 141 (2007).
22. P. Zi, M. C. Zhang, Y. You, D. Y. Geng, J. H. Du, X. L. Ma, Z. D. Zhang. *J. Mater. Sci.* **38**, 689 (2003).
23. C. J. Otten, O. R. Lourie, M.-F. Yu, J. M. Cowley, M. J. Dyer, R. S. Ruoff, W. E. Buhro. *J. Am. Chem. Soc.* **124**, 4564 (2002).
24. T. T. Xu, J.-G. Zheng, N. Wu, A. W. Nicholls, J. R. Roth, D. A. Dikin, R. S. Ruoff. *Nano Lett.* **4**, 963 (2004).
25. A. Chakrabarti, T. Xu, L. K. Paulson, K. J. Krise, J. A. Maguire, N. S. Hosmane. *J. Nanomater.* Article ID 589372 (2010).
26. T. I. Serebryakova, V. I. Lyashenko, V. D. Levandovskii. *Powder Metallurgy Metal Ceram.* **33**, 49 (1994).
27. P. Marmottant, S. Hilgenfeldt. *Nature* **423**, 153 (2003).
28. S. Rooney. In *Other Nonlinear Acoustic Phenomena in Ultrasound: Its Chemical, Physical, and Biological Effects*, S. Suslick (Ed.), VCH, New York (1988).

29. T. Scopigno, U. Balucani, A. Cunsolo, C. Masciovecchio, G. Ruocco, F. Sette, R. Verbeni. *Europhys. Lett.* **50**, 189 (2000).
30. A. Chakrabarti, S. Stanley, K. Boblack, N. S. Hosmane. To be submitted for publication.
31. S.-Y. Xie, W. Wang, K. A. S. Fernando, X. Wang, Y. Lin, Y.-P. Sun. *Chem. Commun.* 3670 (2005).
32. N. G. Chopra, R. J. Luyken, K. Cherry, V. H. Crespi, M. L. Cohen, S. G. Louie, A. Zettl. *Science* **269**, 966 (1995).
33. (a) N. G. Chopra, A. Zettl. *Solid State Commun.* **105**, 297 (1998); (b) W. Q. Han, J. Mickelson, A. Zettl. *Appl. Phys. Lett.* **81**, 1110 (2002); (c) J. Cumings, A. Zettl. *Solid State Commun.* **129**, 661 (2004).
34. D. Golberg, Y. Bando, K. Kurashima, T. Sato. *Scr. Mater.* **44**, 1561 (2001).
35. (a) A. Loiseau, F. Willaime, N. Demoncy, G. Hug, H. Pascard. *Phys. Rev. Lett.* **76**, 4737 (1996); (b) M. Terrones, W. K. Hsu, H. Terrones, J. P. Zhang, S. Ramos, J. P. Hare, R. Castillo, K. Prassides, K. H. Cheetham, W. Kroto, D. R. M. Walton. *Chem. Phys. Lett.* **259**, 568 (1996).
36. (a) O. R. Lourie, C. R. Jones, B. M. Bartlett, P. C. Gibbons, R. S. Ruoff, W. E. Buhro. *Chem. Mater.* **12**, 1808 (2000); (b) R. Z. Ma, Y. Bando, T. Sato, K. Kurashima. *Chem. Mater.* **13**, 2965 (2001); (c) J. S. Wang, V. K. Kayastha, Y. K. Yap, Z. Y. Fan, J. G. Lu, Z. W. Pan, I. N. Ivanov, A. A. Puretzky, D. B. Geohegan. *Nano Lett.* **5**, 2528 (2005).
37. D. Golberg, Y. Bando, M. Eremets, K. Takemura, K. Kurashima, H. Yusa. *Appl. Phys. Lett.* **69**, 2045 (1996).
38. Y. Chen, M. Conway, J. S. Williams, J. Zou. *J. Mater. Res.* **17**, 1896 (2002).
39. (a) D. Golberg, Y. Bando, W. Han, K. Kurashima, T. Sato. *Chem. Phys. Lett.* **308**, 337 (1999); (b) M. Terauchi, M. Tanaka, K. Suzuki, A. Ogino, K. Kimura. *Chem. Phys. Lett.* **324**, 359 (2000).
40. M. W. Smith, K. C. Jordan, C. Park, J.-W. Kim, P. T. Lillehei, R. Crooks, J. S. Harrison. *Nanotechnology* **20**, 505604 (2009).
41. L. Xu, Y. Peng, Z. Meng, W. Yu, S. Zhang, X. Liu, Y. Qian. *Chem. Mater.* **15**, 2675 (2003).
42. A. Chakrabarti, S. Stanley, J. Price, N. S. Hosmane. To be submitted for publication.
43. C. Zhi, Y. Bando, C. Tang, R. Xie, T. Sekiguchi, D. Golberg. *J. Am. Chem. Soc.* **127**, 15996 (2005).
44. C. Zhi, Y. Bando, C. Tang, S. Honda, K. Sato, H. Kuwahara, D. Golberg. *Angew. Chem., Int. Ed.* **44**, 7932 (2005).
45. S. Pal, S. R. C. Vivekchand, A. Govindaraj, C. N. R. Rao. *J. Mater. Chem.* **17**, 450 (2007).
46. T. Ikuno, T. Sainsbury, D. Okawa, J. M. J. Frechet, A. Zettl. *Solid State Commun.* **142**, 643 (2007).
47. X. Chen, P. Wu, M. Rousseas, D. Okawa, Z. Gartner, A. Zettl, C. R. Bertozzi. *J. Am. Chem. Soc.* **131**, 890 (2009).

